Control Strategy of Parallel SVG on Scott Balance Transformer

Yunbo Gao

School of Automation & Electrical Engineering,
Lanzhou Jiaotong University, Lanzhou 730070, Lanzhou, China

Abstract
For solving the problems of harmonic and reactive power pollution of electrified railway, this paper presents SVG multi-module parallel compensation scheme with scott balance transformer. The paper introduces the working theory and characteristics of scott balance transformer, and studies the detection and control methods of SVG in depth. Single-phase synchronous detection method without phase-locked loop is adopted in the command current detection, this method has the advantages of good real-time ability and high detection precision. The two-state hysteresis and three-state hysteresis current control methods are analyzed in detail. A simulation model with the same simulation parameters is established to test SVG parallel compensation effect of these two control methods. The result shows that these two hysteresis control methods are of good tracking performance and high compensation accuracy. However, in terms of switching frequency, the three-state hysteresis control method is capable of frequency multiplication, which effectively reduces the switching losses and improves the efficiency of SVG parallel compensation effect.
Key words: PARALLEL SVG, SCOTT BALANCE TRANSFORMER, TWO-STATE HYSTERESIS, THREE-STATE HYSTERESIS, FREQUENCY MULTIPLICATION

1. Introduction

As large amounts of harmonic and reactive components are produced during the working process of electric locomotive, these pollution components will have a negative influence on the three-phase AC power system and cause the asymmetry of the three-phase current. As a result, the normal performance of other electric equipments connected to the power grid will be affected [1-3]. The application of Static Var Generator (SVG) is effective to solve these issues in recent years. The standard of railway traction power supply is as follows: single-phase alternating current with the voltage class of 27.5kv and the frequency of 50Hz. Due to high current class, large compensation capacity, and the restrictions by the level of power electronic devices, the compensation ability of single SVG module usually cannot meet the requirement for compensation of electrical railway. Therefore, parallel compensation scheme

using multiple SVG units is an effective way to solve this problem.

2. Compensation theory of SVG

SVG devices are usually installed on the overhead contact system (OCS) side, and the working voltage can reach to hundreds or thousands of volts. The large difference from the 27.5kv voltage which is the standard of railway traction power supply stops the SVG devices from connecting to OCS directly, the transformer must be used to isolate and step down the voltage to realize compensation. The schematic diagram of parallel SVG with N modules for electrical railway is shown in Figure 1.

Two 27.5kv single-phase alternating currents are outputted after the three-phase 110kv or 220kv alternating current from the power grid side flows through the traction substation. These two currents are injected into the OCS system to supply power to the electrical locomotive. So the relationship between the output currents of the two single sides (which are called α side and β side) will directly affect the symmetry of the three-phase current on the power grid side. The parallel SVG studied in this paper can realize compensation for three-phase current via compensation for the two single-phase sides. The single-phase back-to-back topology structure is used in the single SVG compensation module, which is consisted of two single-phase full bridge converters and one DC-side capacitor. The two compensation ports are connected to the OCS through step-down transformers respectively to realize compensation for α side and β side.

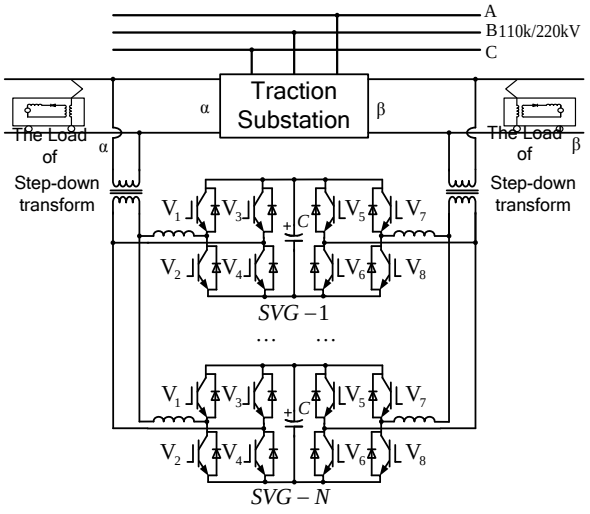

Figure 1. Compensation theory of parallel SVG with N modules

2.1. Scott Transformer

Scott balance transformer is widely used to transform three-phase alternating current to single-phase alternating current in the traction substation of electrical railway. Because of its special inner winding structure, scott balance transformer is capable of keeping the two output voltages at the same amplitude and 90 degree difference in phase. Therefore, scott balance transformer is quite suitable for the supply system for electrical railway. The detailed theory of the transformer is shown in reference [4], this paper will not discuss in depth.

2.2. Specific Functions of SVG

The loads (electric locomotives) on the two output sides (α side and β side) of traction substation are constantly adjusted. In order to make the three-phase current symmetrical without reactive and harmonic components on the power grid side while adopting scott transformer, the condition of $\boldsymbol{I}_\alpha = \mathrm{j}\boldsymbol{I}_\beta$ should be satisfied and the currents should be in phase with the corresponding voltage $\boldsymbol{U}_\alpha$ and $\boldsymbol{U}_\beta$. Thus, SVG for electrical railway should realize three functions at the same time: exchange of active power, harmonic suppression and compensation for reactive power.

3. Current detection method and control strategy of SVG

3.1. Generation of Command Current

In order to compensate OCS system steadily and accurately through SVG devices, the premise is that the component that needs to be compensated must be detected accurately and command current must be calculated precisely. As the power supply pattern of electrical railway is implemented by the transformation from three-phase to single-phase, several common current detection methods are applied, such as single-phase instantaneous reactive power method, phase detection method, single-phase synchronous detection method and so on. The single-phase instantaneous reactive power method has been applied widely, which is developed from the theory proposed by the Japanese scholar Hirofumi Akagi. During the detection process of this method, the virtual three-phase voltage and current are constructed to realize detection of harmonic current. This method not only requires virtual phase, but also phase-locked loop (PLL) and low pass filter (LPF). The method is capable of extracting the fundamental active power, fundamental reactive power and harmonic component respectively, but the calculation process is too complicated and delay time is much longer. While the phase detection method has quite clear principle and easy module, it is also capable of detecting the components of the current respectively, but its accuracy and real-time

performance are poor due to the PLL. The single-phase synchronous detection method is applied in current detection of parallel SVG in this paper, the schematic diagram of the method is shown in Figure 2 [5-7].

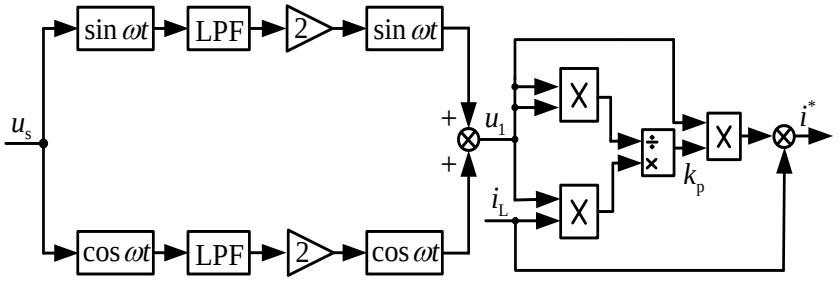

Figure 2. Schematic diagram of the single-phase synchronous detection method

The principle of three-phase synchronous detection method is expressed as follows: the current of each phase has sinusoidal fundamental wave and in phase with the voltage in the ideal three-phase power system. As is in the rotating coordinate system, it shows that the voltage vector co-rotates with the current vector, so this method is called three-phase synchronous detection method. According to the principle mentioned above, it is called single-phase synchronous detection method when applying the detection method for three-phase power system into single-phase power system. Next, the single-phase synchronous detection method will be analyzed in detail according to Figure 2.

In the ideal situation, the linear relationship between the power supply phase voltage u_1 ($u_1 = \sqrt{2}U_1 \sin(\omega t + \phi_1)$) and the power supply phase current i_s can be expressed as follows:

$$i_1 = k_p u_1 \quad (1)$$

Where k_p is the proportional constant.

The power supply active power P_s is expressed as follows:

$$P_s = \frac{1}{T}\int_0^T u_1 i_s \mathrm{d}t = k_p U_1^2 \quad (2)$$

Assume the load current $i_L(t)$ is expressed as follows:

$$i_L(t) = \sqrt{2}I_1 \sin(\omega t + \varphi_1) + \sum_{n=2}^{\infty} \sqrt{2}I_n \sin(n\omega t + \varphi_n) \quad (3)$$

And then, the instantaneous value of load power $p_L(t)$ can be derived:

$$p_L(t) = u_s i_L = \sqrt{2}U_1 \sin(\omega t + \phi_1) \times \left[\sqrt{2}I_1 \sin(\omega t + \varphi_1) + \sum_{n=2}^{\infty} \sqrt{2}I_n \sin(n\omega t + \varphi_n) \right] \quad (4)$$

According to the orthogonality of trigonometric function, the integral value of the product of two trigonometric functions that have the same angular frequency is not equal to zero in one time period T, and the integral value of the product of other signals with different angular frequencies is equal to zero. Therefore, the active power P_L consumed by the load can be derived as follows:

$$P_L = \frac{1}{T}\int_0^T p_L(t)\mathrm{d}t = \frac{1}{T}\int_0^T p_1(t)\mathrm{d}t = \frac{1}{T}\int_0^T u_1 i_1 \mathrm{d}t = U_1 I_1 \cos(\varphi_1 - \phi_1) \quad (5)$$

According to the law of conversation of energy, the active power produced by the power supply should be equal to the active power consumed by the load with losses neglected. Based on Equations (1), (2) and (5), k_p can be derived:

$$k_p = \frac{P_L}{U_1^2} \quad (6)$$

Based on the analysis above, the steps for generating command current can be summed as follows. Firstly, the active power consumed by the load and the proportional constant k_p can be worked out by Equations (5) and (6). Secondly, the fundamental active current i_1 can be derived by Equation(1). Finally, the desired command current i^* can be worked out by subtracting i_1 from the total current. That is the opposite number of the sum of fundamental reactive current and harmonic current.

3.2. Control Strategy of Parallel SVG

For parallel SVG in electrical railway, the research focus is on how to control the on-off state of switching devices of converters to make the actual output current track command current accurately. The common current tracking techniques mainly include hysteresis control method and triangle wave control method. The hysteresis control method is adopted in this paper

due to its high current tracking accuracy, fast dynamic response speed, and the elimination of carrier. In the traditional hysteresis control method, the inverter voltage u_{ab} works in the two states of $+U_{dc}$ and $-U_{dc}$ respectively, so it is called two-state hysteresis control method. However, there are some shortcomings during the control process, such as great current fluctuations, high switching frequency and huge consumption and so on. In this situation, a novel method called three-state hysteresis control method is adopted for the control of parallel SVG in this paper.

As its name implies, three-state hysteresis control method means that the inverter voltage u_{ab} is given three different kinds of state values by introducing zero state in one period time [8-9]. The three values are respectively $+U_{dc}$, 0 and $-U_{dc}$. The schematic diagram is in Figure 3, as a) shows the change of current, b) shows the inverter voltage under two-state hysteresis control, and c) shows the inverter voltage under three-state hysteresis control while the output current is in positive half-cycle.

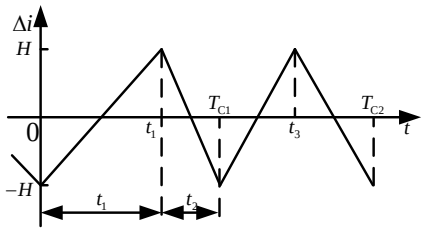

a) Current variation

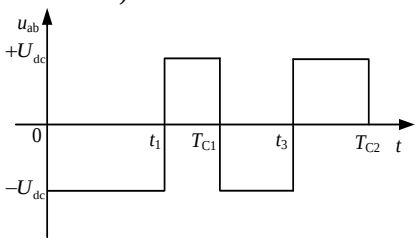

b) AC voltage under two-state hysteresis control

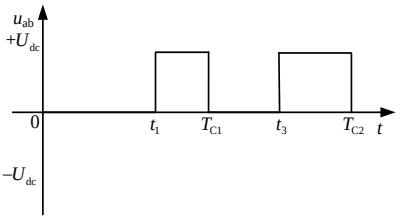

c) AC voltage under three-state hysteresis control ($i_c > 0$)

Figure 3. Schematic diagram of hysteresis control

The control principle of two-state and three-state hysteresis control will be illustrated with the example of single-phase full bridge in the following part. The circuit of single-phase full bridge is shown in Figure 4.

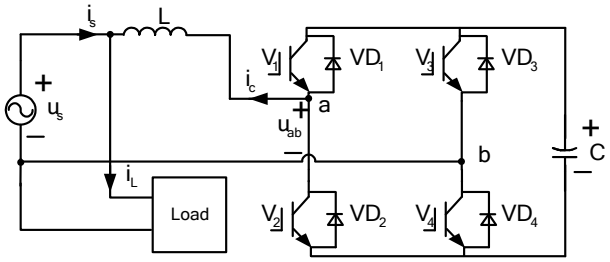

Figure 4. Structure of single-phase full bridge inverter

Assume the current deviation vector Δi is defined as $\Delta i = i^* - i$, combining Figure 3 a) and Figure 3 b), it can be found that single-phase full bridge inverter works in two kinds of state values under two-state hysteresis control. V_1, V_4 are turned on while V_2, V_3 are turned off;

V_2, V_3 are turned on while V_1, V_4 are turned off. In the first state, the value of inverter voltage is $+U_{dc}$. In the second state, the value of inverter voltage is $-U_{dc}$. When $0 < t < t_1$, V_2, V_3 are turned on while V_1, V_4 are turned off, $-H < \Delta i < H$, $u_{ab} = -U_{dc}$. When $t = t_1$, Δi exceeds the set ring width H, the actual current needs to be increased, Δi is decreased and limited steadily within the range of $[-H, H]$ through turning on pulse signal to V_1, V_4 and turning off signal to V_2, V_3. So, when $t_1 < t < t_2$, $u_{ab} = +U_{dc}$. The above process is a complete control period and the state of each switch device changes one time respectively.

The switching frequency under two-state hysteresis control will be analyzed in detail in the following part, the positive direction configuration of current is shown in Figure 4. According to Kirchhoff's voltage law (KVL), Equation (7) is derived:

$$u_s + u_L = U_{dc} \tag{7}$$

Take one switching period T_{c1} as the research object while the inductance voltage is defined as $u_L = L\dfrac{di_L}{dt}$. Substituting Equation (7) into u_L produces:

$$t_1 = \frac{2HL}{U_{dc} - u_s} \tag{8}$$

In the same way, the following can be also derived:

$$t_2 = \frac{-2HL}{-U_{dc} - u_s} = \frac{2HL}{U_{dc} + u_s} \quad (9)$$

According to Equations (8) and (9), the switching frequency f under two-state hysteresis control is calculated as follows:

$$f = \frac{1}{T_{c1}} = \frac{1}{t_1 + t_2} = \frac{U_{dc}^2 - u_s^2}{4HLU_{dc}} \quad (10)$$

As the above shows, the maximum of switching frequency f_{max} (when u_s passes zero) can be derived as follows:

$$f_{max} = \frac{U_{dc}}{4HL} \quad (11)$$

The principle of three-state hysteresis control is analyzed with Figure 3 a) and 3 c). When the output current deviation vector Δi exceeds the ring width H, the actual current i_c is less than the command current i_c^*, the actual current needs to be increased. Specific steps are illustrated as follows. Turn on V_1, V_4 and turn off V_2, V_3 to keep Δi within $[-H, H]$, during this process, $u_{ab} = +U_{dc}$. When the output current deviation vector $\Delta i < -H$, the actual current i is more than the command current i_c^* and exceeds the ring width, the actual current needs to be decreased. The steps are illustrated as follows. Turn on V_1, V_3 and turn off V_2, V_4 to make u_{ab}=0. When $\Delta i \in [-H, H]$, the PWM signal will not be changed and the switching devices will keep the original on-off state. According to the above analysis, the inverter voltage u_{ab} goes through two time periods during one switching period T, it means $t_1 + t_2 = T/2$, so the three-state hysteresis control possesses the capability of frequency multiplication.

The switching frequency under three-state hysteresis control will be analyzed in detail in the following part. As it is similar to the two-state hysteresis control, Equations (12), (13) and (14) can be worked out as follows.

$$t_1 = \frac{2HL}{U_{dc} - u_s} \quad (12)$$

$$t_2 = \frac{-2HL}{-u_s} = \frac{2HL}{u_s} \quad (13)$$

$$\frac{T}{2} = \frac{2HLU_{dc}}{u_s(U_{dc} - u_s)} \quad (14)$$

Then, the switching frequency f can be worked out:

$$f = \frac{1}{T} = \frac{u_s(U_{dc} - u_s)}{4HLU_{dc}} \quad (15)$$

According to Equation (15), f is a quadratic function of the independent variable u_s. Therefore, the maximum switching frequency under three-state hysteresis control is derived:

$$f_{max} = \frac{U_{dc}}{16HL} \quad (16)$$

After comparison between Equation (11) and Equation (16), it is easy to find that three-state hysteresis has better performance than two-state hysteresis with the ring width H, DC voltage and the same AC inductance value L. The maximum switching frequency of the former is only a quarter of the latter.

4. Simulation analysis of parallel SVG

To verify the performance of the detection and control methods studied in this paper, two parallel SVG modules are established and simulated by MATLAB/Simulink.

1) Simulation method. The single-phase synchronous detection method is used to detect current, two-state hysteresis control method and three-state hysteresis control method are used respectively in the control strategy.

2) Simulation parameters. The three-phase voltage on the power grid side is set in Equation (17), the load current on α, β side are set in Equation (18), DC side capacitor C=12.5mF, AC inductance L=0.5mH, the command voltage on DC side is set as $U_{dc}^* = 3300$ V, the hysteresis ring width is set to 12A.

$$\begin{cases} u_a(t) = 5000\sin 100\pi t \\ u_b(t) = 5000\sin(100\pi t - 120^\circ) \\ u_c(t) = 5000\sin(100\pi t + 120^\circ) \end{cases} \quad (17)$$

$$\begin{cases} i_{\alpha L}(t) = 200\sin(100\pi t + 90^\circ) + 300\sin 100\pi t + 30\sin 300\pi t \\ i_{\beta L}(t) = 300\sin 100\pi t + 150\sin(100\pi t + 90^\circ) + 50\sin 400\pi t \end{cases} \quad (18)$$

The simulation waveforms based on the simulation methods and simulation parameters are set as follows:

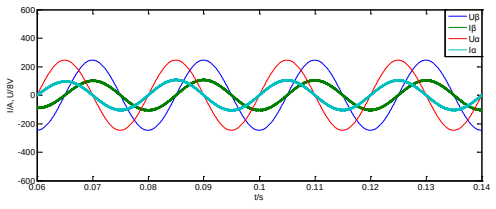

a) Output voltage, current of scott transformer under two-state hysteresis control

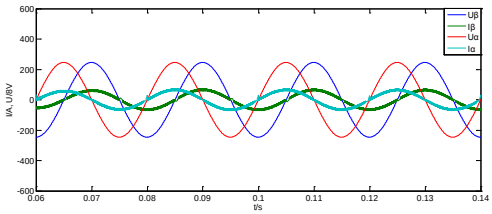

b) Output voltage, current of scott transformer under three-state hysteresis control

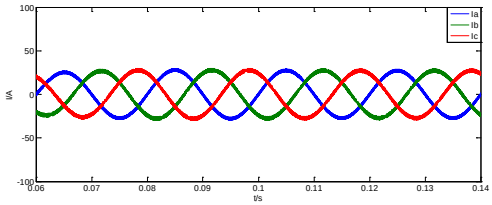

c) Three-phase current on the power grid side under two-state hysteresis control

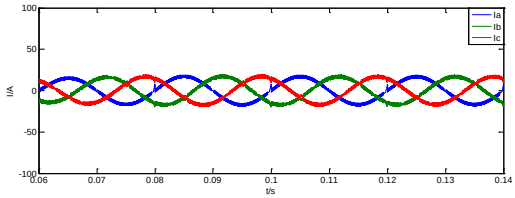

d) Three-phase current on the power grid side under two-state hysteresis control

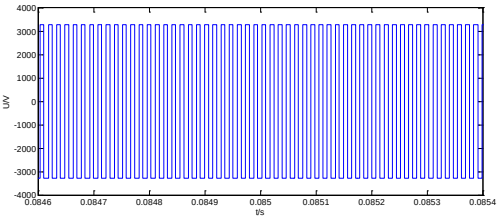

e) Inverter voltage u_{ab} under two-state hysteresis control

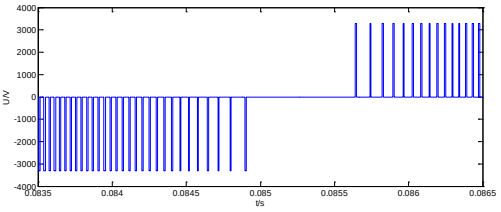

f) Inverter voltage u_{ab} under three-state hysteresis control

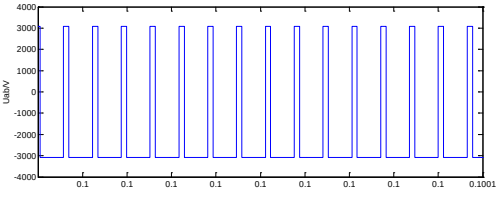

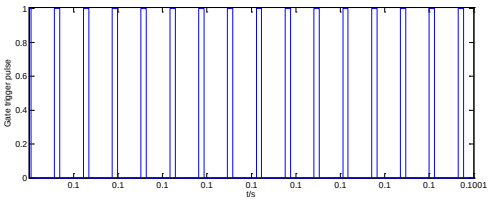

g) Comparison between inverter voltage and drive pulse under two-state hysteresis control

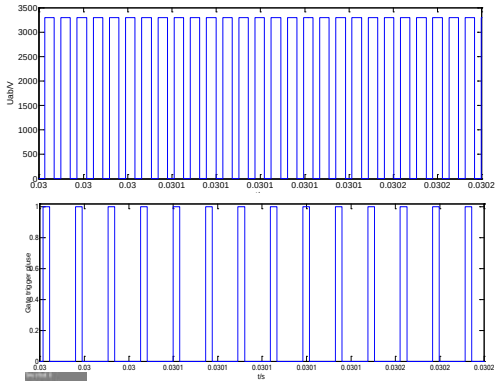

h) Comparison between inverter voltage and drive pulse under three-state hysteresis control

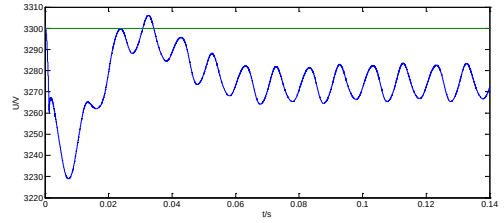

i) DC voltage u_{dc} under two-state hysteresis control

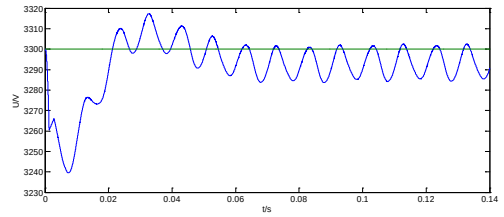

j) DC voltage u_{dc} under three-state hysteresis control

Figure 5. Simulation waveforms

The output voltage u_α, u_β and output current i_α, i_β of scott balance transformer under two-state hysteresis control method and three-state hysteresis control method are shown in Figure 5 a) and Figure 5 b) respectively. It can be found that the expected compensation effect is achieved under both hysteresis control strategies. The current satisfies the condition $\boldsymbol{I}_\alpha = \mathrm{j}\boldsymbol{I}_\beta$ and they are in phase with the corresponding output voltage. According to the previous analysis in this paper, when the current and voltage of scott balance transformer meet the above requirements, the three-phase current on the power grid side is symmetrical. The initially expected compensation

is verified by the simulation waves shown in Figure 5 c) and Figure 5 d).

The local amplification waveforms of inverter voltage u_{ab} under two-state hysteresis control method and three-state hysteresis control method are shown respectively in Figure 5 e) and Figure 5 f), it can be observed that under the two-state hysteresis control method, the value of u_{ab} have two states, , namely +3300V and -3300V. Under the three-state hysteresis control method, the value of u_{ab} have three states, namely +3300V, 0V and -3300V. In order to compare the frequency relationship between inverter voltage and gate trigger pulse under these two hysteresis control methods, the gate signal of one switching device of parallel SVG is taken as reference. The simulation waveforms are shown in Figure 5 g) and Figure 5 h) respectively. The frequencies of inverter voltage and gate trigger pulse are the same under the two-state hysteresis control method; however, the frequency of inverter voltage is twice the frequency of gate trigger pulse under the three-state hysteresis control method. Therefore, the three-state hysteresis control method has the capability of frequency multiplication, this will help to reduce the switching losses and improve the compensation efficiency of parallel SVG.

Finally, the control performance on DC side voltage u_{dc} under these two hysteresis control methods is observed and illustrated in Figure 5 i) and Figure 5 j). It can be found that DC side voltage is limited to 3280V while the command voltage is 3300 V under the two-state hysteresis control method, the deviation ratio is $(3300-3280)/3300 \approx 0.61\%$. DC side voltage is limited to 3295V under the three-state hysteresis control method, the deviation ratio is $(3300-3295)/3300 \approx 0.15\%$ and gradually decreases along with the extension of simulation time.

5. Conclusions

This paper studies the control strategy of SVG parallel compensation device applied in the electrical railway. The scott balance power supply pattern is used in the traction substation, and the single-phase synchronous detection method is applied in the detection of command current. The two-state hysteresis control method and three-state hysteresis control method are used in the control strategy respectively. The conclusions are drawn as follows:

1) The scott balance transformer is suitable in the three-phase and single-phase power supply pattern of electrical railway, the three-phase voltage and current on the power grid side are symmetrical when the following conditions are met, namely $\boldsymbol{I}_{\alpha}=\mathrm{j}\boldsymbol{I}_{\beta}$, 90 degree difference in phase and the currents be in phase with the corresponding voltage $\boldsymbol{U}_{\alpha}$ and $\boldsymbol{U}_{\beta}$.

2) The single-phase synchronous detection method has clear principle and is easy to implement without PLL modules. Therefore, the good real-time performance makes it an effective method to be applied to the current detection for parallel SVG.

3) The two-state hysteresis control method and three-state hysteresis control method are suitable for the control of parallel SVG due to the ideal control accuracy. The three-state hysteresis control method is capable of frequency multiplication under the same control conditions, which will help to reduce the switching losses, it has better compensation efficiency than two-state hysteresis control method.

References

1. Chi Sun, Guanghui Wei, Zengjun Bi (2003) Detection of reactive power and harmonic current of three-phase asymmetrical system based on synchronous reference frame. *Proceedings of CSEE*, 23(12), p.p.43-48.
2. Herong Gu, Zilong Yang, Weiyang Wu (2006) Research on hysteresis-band current tracking control of grid-connected inverter. *Proceedings of CSEE*, 26(9), p.p.108-112.
3. Kexin Wei, Shujun Zhang (2005) Novel 3-phase voltage source converters with hysteresis current control. *Relay*, 33(16), p.p.58-61.
4. Lei K., An L., Chuanping W. (2013) A novel power quality compensation device based on two-phase three-wire converter for high speed electric railway. *Power system technology*, 37(1), p.p.67-78.
5. Ohmi M, Yoshi Y. (2010) Validation of railway static power conditioner in Tohoku Shinkansen on actual operation. *Power Electronics Conference(IPEC)*, Sapporo, Japan, p.p.678-684.
6. Shaofeng Xie, Qunzhan Li, Liping Zhao (2005) Study on harmonic distribution characteristic and probability model of the traction load of electrified railway. *Proceedings of the CSEE*, 25(16), p.p.79-83.
7. Xiangning Xiao, Minxiao Han, Yonghai Xu (2004) *Control and analysis of power quality*. China Electric Power Press: Beijing.
8. Xin Tang, An Luo (2009) Three-state hysteresis control method of active power filter based on repeating prediction. *Transactions of china electrotechnical society*, 24(9), p.p.134-138.

9. Xin Z., Quanyuan J. (2014) Capacity configuration of V/V transformer-based railway power conditioner and optimal energy compensation strategy. *Electric power automation equipment*, 34(1), p.p.92-99.
10. Yangfan Ou (2008) Research on a Single-Phase to Three-Phase Power Supply Method Based on Balance Transformer. *Transactions of China Electrotechnical Sosiety*, 23(9), p.p.132-137.